

Extending Fluorescence of *meso*-Aryldipyririn Indium(III) Complexes to Near-Infrared Regions via Electron Withdrawing or π -Expansive Aryl Substituents

Levi Lystrom, Manoj Shukla, Wenfang Sun, and Svetlana Kilina*

Cite This: *J. Phys. Chem. Lett.* 2021, 12, 8009–8015

Read Online

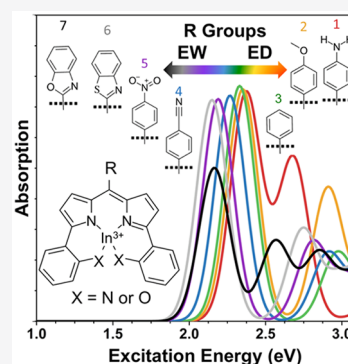
ACCESS |

Metrics & More

Article Recommendations

Supporting Information

ABSTRACT: The absorption and fluorescence spectra of 14 In(III) dipyririn-based complexes are studied using time-dependent density functional theory (TDDFT). Calculations confirm that both heteroatom substitution of oxygen (N_2O_2 -type) by nitrogen (N_4 -type) in dipyririn ligand and functionalization at the *meso*-position by aromatic rings with strong electron-withdrawing (EW) substituents or extended π -conjugation are efficient tools in extending the fluorescence spectra of In(III) complexes to the near-infrared (NIR) region of 750–960 nm and in red-shifting the lowest absorption band to 560–630 nm. For all complexes, the emissive singlet state has π - π^* character with a small addition of intraligand charge transfer (ILCT) contributing from the *meso*-aryl substituents to the dipyririn ligand. Stronger EW nitro group on the *meso*-phenyl or *meso*-aryl group with extended π -conjugation induces red-shifted electronic absorption and fluorescence. More tetrahedral geometry of the complexes with N_4 -type ligands leads to less intensive but more red-shifted fluorescence to NIR, compared to the corresponding complexes with N_2O_2 -type ligands that have a more planar geometry.



Discovery of new near-infrared (NIR) absorbing and emissive materials is critical for applications in fluorescent biomarkers,¹ photodynamic therapy (PDT),^{2,3} fluorescent sensors,⁴ photovoltaics,^{5–8} and light emitting diodes (LEDs).^{9,10} Metal centered dipyrromethene (M-DIPYs) and azadipyrromethenes (M-aza-DIPYs) are classes of organometallic complexes that have received significant attention in recent years due to their promising optical properties, which can be extended to the NIR region.^{4,10–15} M-DIPY ligands can be easily functionalized on the α - and β -positions of pyrrole rings as well as at the *meso* position.^{16–20} Such functionalization provides means for the tuning of electronic properties and shifting the absorption and emission of the complexes into the NIR region.^{17,18,20,21}

The N_2O_2 -type dipyririns are particularly interesting as tetra-coordinated ligands, since they increase the structural rigidity of the complexes. It is known that structural rigidity helps to suppress nonradiative pathways and is a key factor for highly emissive NIR materials.²² The incorporation of Group-13 and -14 elements into the N_2O_2 -type *meso*-aryldipyririns (N_2O_2 -type) ligand is known to result in stable complexes emitting in the deep-red spectral region.^{10,13} Among these complexes, the most efficient emitter is an In(III) complex containing *meso*-mesityl- N_2O_2 -DIPY ligand, which exhibits a fluorescence quantum yield (QY) of 67% at 639 nm.¹³ So far, this is the highest emission QY reported for In(III) dipyririn complexes. Despite this promising result, reports on the functionalization of the In(III) complexes comprising dipyririn derivatives are limited and lack concise and systematic approaches to tuning

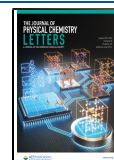
and improving their optical response. As such, there is a gap in an understanding of the structure–property relationship for rational design of Group-13 metal–organic complexes with targeting optical properties.

Since ligand functionalization by electron donating (ED) and withdrawing (EW) groups or groups with extended π -conjugation is known as a powerful tool for tuning and improving the optical response of Ir(III), Ru(II), Pt(II), and other metal–organic complexes,^{23–31} we performed computational studies of these substituent effects on dipyririn In(III) complexes in order to understand how to shift their absorption and emission bands toward the NIR region. As depicted in Scheme 1, we consider two derivatives of dipyririn In(III) complexes, the N_2O_2 - and N_4 -type, where the N_4 -type is different from the N_2O_2 -type by replacing the coordinated oxygens with nitrogens. The substituting aryl groups at the *meso*-position of N_2O_2 -type (series a) and N_4 -type (series b) are chosen to gradually increase the pull-push effect of the substituent at the 4-phenyl position from ED groups in 1 and 2 to EW groups in 4 and 5. Meanwhile, the effects of the expanded π -conjugation of the *meso*-aryl group and the increased coplanarity between the *meso*-aryl group and the

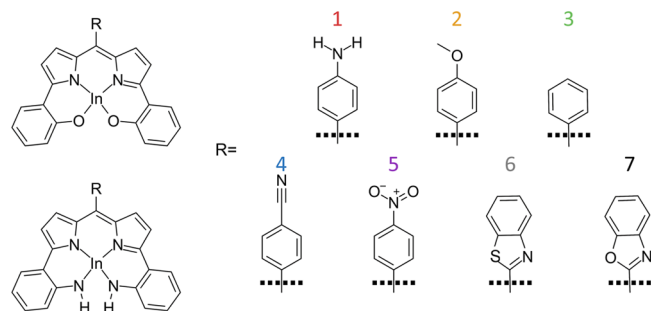
Received: July 3, 2021

Accepted: August 9, 2021

Published: August 16, 2021



Scheme 1. In(III) Complexes with N₂O₂-Type (Series a) or N₄-Type (Series b) Dipyrrin Ligands Containing Different *meso*-Aryl Substituents^a



^aThe electron-withdrawing ability of the substituent at the 4-position of the *meso*-phenyl group increases from complex 1 to 5, and π -conjugation is extended in complexes 6 and 7.

dipyrrin component are evaluated with a comparison of the complexes 6 and 7 to 3.

The synthesis of the N₂O₂-type ligands and their coordination to Group-13 and -14 metals has been reported in literature.^{9,10,13,32–34} However, there are no reports on the coordination of N₄-type dipyrrin ligands to In(III). Due to the stronger electron-donating ability of nitrogens compared to oxygens, we expect that replacing oxygens in N₂O₂-type by nitrogens in N₄-type will impact both the absorption and emission features of the In(III) complexes and red-shift the optical spectra. To our knowledge, no studies investigating the effect of EW/ED substituent groups on N₂O₂- and N₄-type dipyrrin ligands have been published yet for In(III) complexes.

The geometries of all complexes were optimized with density functional theory (DFT) using the PBE0³⁵ functional and the mixed basis sets with LANL2DZ³⁶ assigned to In(III) and 6-31G* to all other atoms,^{37,38} utilizing Gaussian-16 software package.³⁹ All calculations were performed in acetonitrile solvent incorporated via Conductor Polarized Continuum Model (CPCM).^{40,41} As a reference point, the calculated geometry of complex 3a is in good agreement with the reported X-ray crystallographic data for an In(III) *meso*-mestyl-N₂O₂ complex.¹³ Substitution of oxygen in N₂O₂-type by nitrogen results in a more tetrahedral structure of N₄-type In(III) complexes, compared to the distorted square planar structure of N₂O₂-type In(III) complexes, as demonstrated by the bond angles between the coordinating pyrrole nitrogen atoms and the trans-oxygen (nitrogen) atoms on the phenyl rings, Table S1 in SI.

The shift in the energy of the lowest absorption band can be qualitatively predicted by the stabilization or destabilization of the frontier molecular orbitals (MOs).^{42–44} As shown in Figures 1a and S1a, the HOMO–LUMO gap increases with the strength of the ED groups from complex 3 to 1 and decreases with the strength of the EW groups in 4 and 5 for both series-a and -b complexes, respectively. This trend is also followed by complexes 6 and 7, showing that extended π -conjugation in the substituent groups leads to reduction of the energy gap. Meanwhile, series-b complexes with N₄-type ligand result in smaller energy gaps by 0.12–0.15 eV compared to their respective complexes in series-a with N₂O₂-type ligand.

For all complexes, the reduction of the HOMO–LUMO gap by EW group or extended π -conjugation is governed by stabilization of the LUMO energies, while the HOMO energies

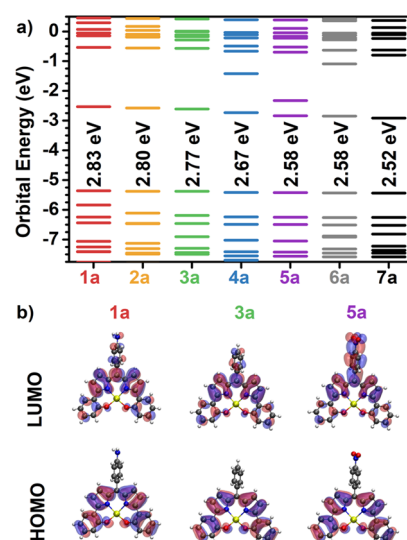


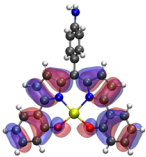
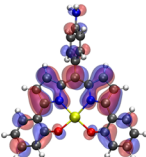
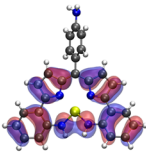
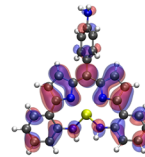
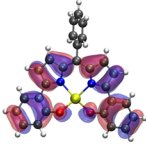
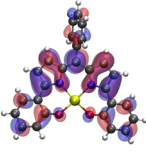
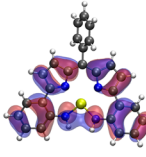
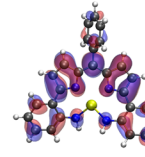
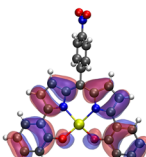
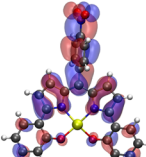
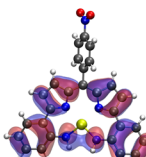
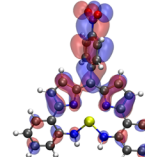
Figure 1. (a) Ground-state molecular orbital diagram for complexes 1a–7a and (b) visualization of HOMO and LUMO for the complexes 1a, 3a and 5a with the strongest ED group, neutral, and the strongest EW group on the *meso*-phenyl rings, respectively. The solvent used for the calculation was acetonitrile.

are not affected by the ED/EW abilities or π -conjugation of the *meso*-aryl substituents. The insensitivity of HOMO to *meso*-aryl substituents is rationalized by its localization on the N₂O₂-type or N₄-type ligands rather than on the *meso*-aryl substituents (see the molecular orbital plots in Figures 1b and S1b). In contrast, the LUMO is delocalized over the entire complex, including the *meso*-aryl substituents. Consequently, ED group destabilizes the LUMO, while the EW group or the more π -conjugated aryl substituent stabilizes the LUMO.

Among all complexes, 5a and 5b exhibit the largest portion of the LUMO on their 4-NO₂-phenyl substituent group, while its delocalization over the N₂O₂-DIPY or N₄-DIPY components is slightly reduced. This leads to the strongest stabilization of their LUMO. The π -conjugation of the *meso*-aryl substituents in complexes 6a, 7a and 6b, 7b hybridizes the electronic density over the entire ligand, while their LUMOs are strongly stabilized having energy that is nearly the same as those of 5a and 5b (Figures 1b and S1b). Interestingly, the LUMO+1 of complexes with EW groups on the phenyl ring or more π -conjugated *meso*-substituents (4–7) is mainly localized on the *meso*-substituents with a small admixture to the dipyrrin ligand, while this trend is reversed in complexes 1–3 that have ED groups or no substituent on the phenyl rings (Tables S2 and S3). This trend is consistent with the ED or EW nature of the 4-substituents on the phenyl rings.

Since there are a large energy gaps separating the frontier orbitals (HOMO and LUMO) from other MOs, we expect that the first excited state is comprised primarily a transition from HOMO to LUMO with a predominant π – π^* nature due to significant electron density distribution of both HOMO and LUMO over the dipyrrin ligands. Meanwhile, intraligand charge transfer (ILCT) also should make considerable contribution to the lowest-energy transition because of the delocalization of electron density to the *meso*-aryl substituents, with the largest ILCT degree in complexes 4 and 5 that bear EW group on the *meso*-phenyl substituents. Thus, the energy of the first optical transition is expected to be red-shifted with increasing the strength of EW groups or extended π -

Table 1. NTOs Showing the Electron-Hole Pair Contribution to the Lowest Energy Transition (S_1) in Absorption Spectra Calculated in Acetonitrile for Complexes with the Strongest Electron Donating (1a and 1b) and Withdrawing (5a and 5b) Groups and the “Neutral” Aryl Group (3a and 3b)

| | Hole | Electron | | Hole | Electron |
|------------------------------------|---|---|------------------------------------|--|---|
| 1a 2.37 eV $f = 0.65$ |  |  | 1b 2.17 eV $f = 0.51$ |  |  |
| 3a 2.33 eV $f = 0.67$ |  |  | 3b 2.15 eV $f = 0.51$ |  |  |
| 5a 2.16 eV $f = 0.44$ |  |  | 5b 1.96 eV $f = 0.25$ |  |  |

conjugation of the *meso*-aryl substituents, following the trend of the HOMO–LUMO gap of these complexes.

This trend has been testified in both series **a** and **b** complexes, as evidenced by the maximum difference of 0.22 eV between complexes **1** and **7** for their lowest-energy optical transitions (see S_1 state energies in Table 1 and Tables S4 and S5 in SI), and is further illustrated by the electronic absorption spectra shown in Figure 2. Similar to the trend of HOMO–LUMO energy gaps observed in the corresponding series-a and -b complexes, the absorption spectra of N_4 -type In(III) complexes in series-b are red-shifted by ~ 0.2 eV with respect to their corresponding N_2O_2 -type In(III) complexes in series-a. As such, the effect of replacing oxygens in the N_2O_2 -type ligand by nitrogens is comparable to that of strong EW groups or π -expansive *meso*-aryl substituents, with both leading to noticeable red-shifts of the absorption spectra and resulting in the most red-shifted lowest-energy absorption band at <2.0 eV in complexes **5b** and **7b**, Figure 2.

The presented absorption spectra in Figure 2 were calculated using liner response time-dependent DFT (TD-DFT)⁴⁵ and the same methodology as that applied to ground-state calculations. It is worth noting that to justify our computational method, we compared the calculated absorption spectrum of **3a** to the experimental spectrum of an In(III) complex with a *meso*-mesityl N_2O_2 -DIPY ligand (which is a complex analogous to **3a**) reported by Sumiyoshi, et al.;¹³ Figure S2 in SI. Except the constant blue-shift (~ 0.3 eV), the calculations well reproduce the main optical features observed in the experimental spectrum. The blue-shift is attributed to vibronic effects that are missed in TDDFT calculations, solvent effects that are not completely introduced by the polar media model for pure solvents, and mesityl group in the *meso*-position of N_2O_2 -dipyrin complex studied experimentally instead of phenyl group in the calculated **3a** complex.

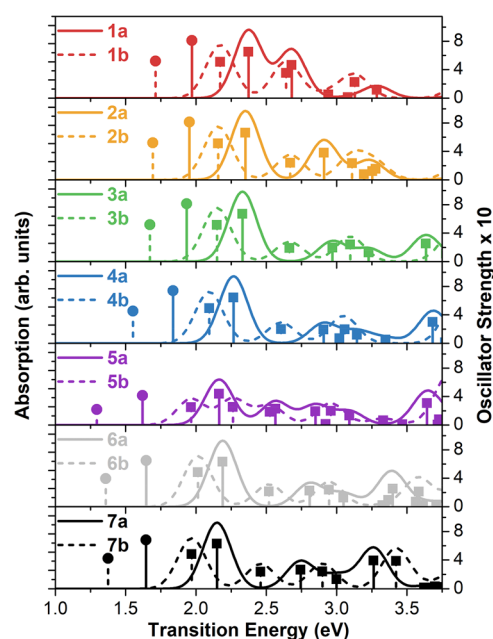
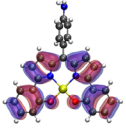
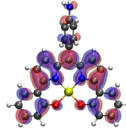
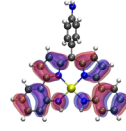
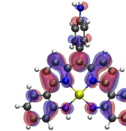
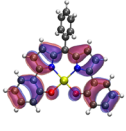
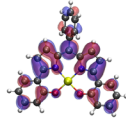
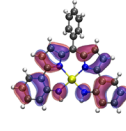
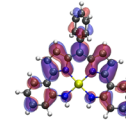
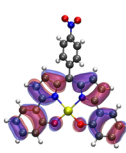
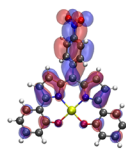
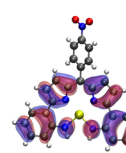
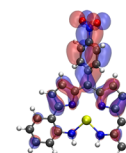


Figure 2. Simulated absorption spectra and emission energies for **1a**–**7a** (solid lines) and **1b**–**7b** (dashed lines) in acetonitrile. The vertical lines with filled boxes or circles represent optical transitions contributing to the absorption bands or emission, respectively.

To represent each excitation as an electron–hole pair, natural transition orbital (NTO) analysis was performed by applying unitary transformation of transition density matrix of a specific excited state.⁴⁶ In particular, as shown in Table 1, NTOs contributing to S_1 are very similar in nature to the ground-state HOMO and LUMO exhibiting mainly π – π^* character admixing with some ILCT, which results in an optically active S_1 state. The only complexes with diminished

Table 2. NTOs Showing the Electron-Hole Contribution to the Singlet Emissive State Calculated in Acetonitrile for Complexes with the Strongest Electron Donating (1a and 1b) and Withdrawing (5a and 5b) Groups and the “Neutral” Aryl Group (3a and 3b)

| | Hole | Electron | | Hole | Electron |
|------------------------------------|---|---|------------------------------------|--|---|
| 1a 1.97 eV $f = 0.81$ |  |  | 1b 1.71 eV $f = 0.52$ |  |  |
| 3a 1.93 eV $f = 0.81$ |  |  | 3b 1.67 eV $f = 0.52$ |  |  |
| 5a 1.62 eV $f = 0.41$ |  |  | 5b 1.29 eV $f = 0.22$ |  |  |

optical response are **5a** and **5b**, which can be rationalized by the increased ILCT character due to stronger localization of the electron density at the *meso*-(4-NO₂phenyl) substituent. This significant increase in the charge transfer nature of the lowest exciton in **5a** and **5b**, compared to that of complexes **1–4**, is also evidenced by the deviation from the linear trend of S_1 energy that decreases with increasing Hammett Parameter following the electron accepting ability of the substituents from **1** (ED) to **4** (EW); Figure S3 in SI. In both series-a and -b complexes, higher energy absorption bands are also dominated by $\pi-\pi^*$ transitions with a small admixture of ILCT, while contribution of the metal center to all optically active transitions is negligible, as depicted by NTOs in Tables S4 and S5 in SI.

A comparison of the absorption spectra of corresponding complexes in series-a and -b (Figure 2) reveals that substitution of the coordinating oxygens by nitrogens results in some decrease in optical activity of the S_1 states for all N₄-type In(III) complexes. One possible explanation of this trend is related to the reduced degree of conjugation in series-b complexes caused by their more tetrahedral structures (Table S1) compared to the distorted square-planar geometries of complexes in series-a. Better conjugation of the NO₂-type complexes in series-a results in stronger delocalization of the electron and/or hole wave function all over the conjugated system, which, in turn, increases the probability of wave function overlaps between the electron and hole due to excitation. This is expected to increase the transition dipole moment and, consequently, the oscillator strength of the transition originated from such electron–hole pair.

It has been reported that the observed emission from the In(III) N₂O₂-DIPY complexes is fluorescence from the singlet excited state.¹³ It is reasonable to assume that the emission from complexes **1–7** will also occur from a singlet state

(fluorescence) rather than from a triplet state (phosphorescence). A lack of MLCT character in the lowest optical transition of all studied complexes also points to an insufficient intersystem crossing and more probable emission from a single state, rather than the triplet state in the studied In(III) complexes.

To calculate the fluorescence energies, we used analytical gradient TDDFT (AG-TDDFT)^{47,48} that provides a geometry optimization of the electronic excited state. While accurate simulations of emission processes, including the radiative and nonradiative lifetime, the emission line widths, and the emission QY, require more advanced level of theory based on nonadiabatic excited state dynamics,^{49,50} our calculations are focused solely on the energy of the emissive states as a function of the ED/EW ability or π -extension of the substituting groups. The AG-TDDFT has been shown sufficient for providing reasonable results on emission energies of Ir(III) complexes.^{26,51,52} The calculated emission energy of the complex **3a** also perfectly agrees with the experimental value of 1.94 eV for the *meso*-mesityl-N₂O₂-DIPY complex.¹³

Figure 2 shows the fluorescence energies of complexes **1–7**. The Stokes shifts are larger for complexes in series-b (ca. 0.5–0.7 eV) compared to those of complexes in series-a (ca. 0.4–0.5 eV) and increase with the EW strength of the substituents on the *meso*-phenyl groups and with the extended π -conjugation of the *meso*-aryl substituents. Note that the calculated Stokes shift is overestimated for **3a** (~0.4 eV), compared to the experimental value (~0.1 eV), which might be explained by the more polar solvent used in calculations, while also missing the solvent reorganization effect due to the implicit description of a solvent via an average polar media. The more planar structures of complexes in series-a provide a stronger conjugation in the N₂O₂-type ligand and prevent substantial geometric changes upon photoexcitation, ration-

alizing the smaller Stokes shifts of complexes in series-a compared to the corresponding complexes in series-b that have a more tetrahedral geometry, as shown in Tables S1 in SI.

For complexes in both series-a and -b, the fluorescence energies follow the trend of the lowest-energy absorption band, i.e., the emission energy is reduced with increasing the EW strength of the substituents on the *meso*-phenyl groups or extending the π -conjugation of the *meso*-aryl substituents. However, compared to the lowest-energy absorption band, this red-shift is more pronounced for fluorescence energies, resulting in a maximum of ~ 0.4 eV fluorescence red-shift between complexes **1** with the strongest ED substituent group and complexes **5** with the strongest EW substituent group. Similar to absorption, the emission energies of all complexes in series-b are lower compared to those of corresponding complexes in series-a by about 0.3 eV. Similarities in absorption and emission trends are rationalized by the nearly unchanged character of the lowest singlet exciton density upon its relaxation, as can be seen from comparison of the NTOs presented in Table 1 (optimized ground-state geometry) and Table 2 (optimized excited-state geometry) and Tables S6 and S7 in SI for singlet and triplet states for all complexes. The triplet excitons, T_1 , have similar character as singlets, except increased π - π^* and reduced ILCT characters in complexes **4** and **5** with strong EW groups.

The combination of replacing oxygen atoms by nitrogen atoms in dipyrroin ligands and its functionalization by the strongest EW substituent on the *meso*-phenyl or extending the π -conjugation of the *meso*-aryl group shifts the emissive singlet states of **5b–7b** to the NIR region of ca. 900–960 nm. However, the oscillator strengths (f) of these emissive S_1 states in complexes with N_4 -type ligands are noticeably lower than those with N_2O_2 -type ligands. According to Kasha's rule,⁵³ the fluorescence occurs in appreciable yield only from the lowest excited state S_1 . The Einstein A and B coefficients can be used to estimate the radiative rate (A), which is proportional to the oscillator strength of the lowest transition.⁵⁴ As such, a small f value of S_1 state suggests a higher chance of nonradiative decay processes outperforming the radiative one and thus quenching the emission.

Thus, the oscillator strength of the lowest-energy transition can be used as a qualitative estimate of the emission efficiency. Since the oscillator strengths of the emissive states in complexes **1b–7b** are about two times lower than those in their corresponding complexes **1a–7a** (Tables 2 and S6), it is expected that the fluorescence QYs of **1b–7b** are lower than those of **1a–7a**. Also, reduced fluorescence QYs in **1b–7b** are expected because the emitting state energies of **1b–7b** (1.29–1.71 eV, i.e. 725–961 nm) are significantly lower than those of **1a–7a** (1.62–1.97 eV, i.e. 629–765 nm). According to the energy-gap law,⁴⁹ the nonradiative decay rate increases exponentially with the reduced emitting state energy. Consequently, the emission QY will be reduced when the emitting state energy is lowered. Alternatively, the effect of significant changes toward flattened geometry at the excited states in **1b–7b** (Table S1) on their fluorescence QYs cannot be excluded.

In summary, our calculations predict that both the substitution of oxygen to nitrogen atoms in dipyrroin and its functionalization at the *meso*-position by strong EW groups on the phenyl rings or expansion of the π -conjugation of the aryl substituents are efficient tools in extending the emission energies of In(III) complexes to the NIR region of 750–960

nm, and in red-shifting the lowest-energy absorption band to 560–630 nm. For all In(III) complexes investigated in this work, regardless of the N_2O_2 -type or N_4 -type series, the lowest singlet exciton contributing to the lowest-energy absorption band or fluorescence mainly has a π - π^* nature admixing with some ILCT character, resulting in the optically active state. For these excitons, the holes are localized on the dipyrroin core, while the electrons are spread over the dipyrroin core and the *meso*-aryl substituents, with the latter attracting slightly more electron density upon increasing the EW ability of the substituent on the *meso*-phenyl group or expanding the π -conjugation of the *meso*-aryl substituent. Such an electron distribution of the S_1 state is responsible for the red-shifted lowest-energy absorption bands and fluorescence in complexes **4a–7a** and **4b–7b**.

While the In(III) N_4 -type complexes with strong EW substituent or extended π -system on the *meso*-aryl group (**5b–7b**) show the most red-shifted fluorescence, the oscillator strength of the transition contributing to fluorescence is relatively weak, which wanes the conditions for high fluorescent QYs. This behavior can be attributed to more pronounced geometry changes from the ground state to the excited state of all complexes with N_4 -type ligand, while it also satisfies the energy-gap law. Taking into account both the fluorescence energy and QY, complexes **5a–7a** with the N_2O_2 -type ligands may be better candidates for applications that require emission at ca. 750 nm. However, for applications that demand emission in the region of >900 nm, **5b–7b** with the N_4 -type ligands would be better choices. Overall, the NIR fluorescence from these complexes makes them promising for potential applications in night-vision-readable displays, light-emitting diodes, telecommunication, optical sensing, photocatalysis, and bioimaging.

■ ASSOCIATED CONTENT

Supporting Information

The Supporting Information is available free of charge at <https://pubs.acs.org/doi/10.1021/acs.jpclett.1c02150>.

Description of the material included; molecular orbitals diagram and electron density distribution, structural parameters, images of the optimized ground-state and excited-state geometries of all studied complexes, experimental and calculated spectra of **3a** complex; dependence of several calculated photophysical properties of complexes **1–5** on Hammett constant; NTOs contributing to main absorption bands and singlet and triplet emission of complexes **1a–7a** and **1b–7b** (PDF)

■ AUTHOR INFORMATION

Corresponding Author

Svetlana Kilina – Department of Chemistry and Biochemistry, North Dakota State University, Fargo, North Dakota 58108, United States; orcid.org/0000-0003-1350-2790; Email: Svetlana.Kilina@ndsu.edu

Authors

Levi Lystrom – Environmental Laboratory, U.S. Army Engineer Research and Development Center, Vicksburg, Mississippi 39180, United States; Oak Ridge Institute for Science and Education, Oak Ridge, Tennessee 37830, United States; Department of Chemistry and Biochemistry, North

Dakota State University, Fargo, North Dakota 58108, United States; orcid.org/0000-0001-6369-8643

Manoj Shukla – Environmental Laboratory, U.S. Army Engineer Research and Development Center, Vicksburg, Mississippi 39180, United States; orcid.org/0000-0002-7560-1172

Wenfeng Sun – Department of Chemistry and Biochemistry, North Dakota State University, Fargo, North Dakota 58108, United States; orcid.org/0000-0003-3608-611X

Complete contact information is available at:

<https://pubs.acs.org/10.1021/acs.jpclett.1c02150>

Notes

The authors declare no competing financial interest.

ACKNOWLEDGMENTS

This work was financially supported by the National Science Foundation (CHE-1800476) to W. Sun and S. Kilina. This work used resources of the Center for Computationally Assisted Science and Technology (CCAST) at North Dakota State University, which were made possible in part by NSF MRI Award No. 2019077.

REFERENCES

- (1) Florès, O.; Pliquett, J.; Abad Galan, L.; Lescure, R.; Denat, F.; Maury, O.; Pallier, A.; Bellaye, P.-S.; Collin, B.; Mème, S. Aza-BODIPY Platform: Toward an Efficient Water-Soluble Bimodal Imaging Probe for MRI and Near-Infrared Fluorescence. *Inorg. Chem.* **2020**, *59*, 1306–1314.
- (2) Dougherty, T. J.; Gomer, C. J.; Henderson, B. W.; Jori, G.; Kessel, D.; Korbek, M.; Moan, J.; Peng, Q. Photodynamic Therapy. *J. Natl. Cancer Inst.* **1998**, *90*, 889–905.
- (3) Wang, C.; Lystrom, L.; Yin, H.; Hetu, M.; Kilina, S.; McFarland, S. A.; Sun, W. Increasing the Triplet Lifetime and Extending the Ground-State Absorption of Biscyclometalated Ir(III) Complexes for Reverse Saturable Absorption and Photodynamic Therapy Applications. *Dalton Trans.* **2016**, *45*, 16366–16378.
- (4) Sakamoto, N.; Ikeda, C.; Yamamura, M.; Nabeshima, T. Structural Interconversion and Regulation of Optical Properties of Stable Hypercoordinate Dipyrin–Silicon Complexes. *J. Am. Chem. Soc.* **2011**, *133*, 4726–4729.
- (5) Shimizu, S.; Iino, T.; Saeki, A.; Seki, S.; Kobayashi, N. Rational Molecular Design towards Vis/NIR Absorption and Fluorescence by using Pyrrolopyrrole aza-BODIPY and its Highly Conjugated Structures for Organic Photovoltaics. *Chem. - Eur. J.* **2015**, *21*, 2893–2904.
- (6) Xie, B.; Chen, Z.; Ying, L.; Huang, F.; Cao, Y. Near-Infrared Organic Photoelectric Materials for Light-Harvesting Systems: Organic Photovoltaics and Organic Photodiodes. *InfoMat* **2020**, *2*, 57–91.
- (7) Singh, S. P.; Gayathri, T. Evolution of BODIPY Dyes as Potential Sensitizers for Dye-Sensitized Solar Cells. *Eur. J. Org. Chem.* **2014**, *2014*, 4689–4707.
- (8) Li, M.; Kou, L.; Diaol, L.; Zhang, Q.; Li, Z.; Wu, Q.; Lu, W.; Pan, D.; Wei, Z. Theoretical Study of WS-9-Based Organic Sensitizers for Unusual Vis/NIR Absorption and Highly Efficient Dye-Sensitized Solar Cells. *J. Phys. Chem. C* **2015**, *119*, 9782–9790.
- (9) Ikeda, C.; Ueda, S.; Nabeshima, T. Aluminium Complexes of N₂O₂-Type Dipyrins: The First Hetero-Multinuclear Complexes of Metallo-Dipyrins with High Fluorescence Quantum Yields. *Chem. Commun.* **2009**, 2544–2546.
- (10) Yamamura, M.; Albrecht, M.; Albrecht, M.; Nishimura, Y.; Arai, T.; Nabeshima, T. Red/Near-Infrared Luminescence Tuning of Group-14 Element Complexes of Dipyrins Based on a Central Atom. *Inorg. Chem.* **2014**, *53*, 1355–1360.
- (11) Makarova, E. A.; Zatsikha, Y. V.; Newman, K. M.; Paidi, V. K.; Beletsky, V. A.; Van Lierop, J.; Lukyanets, E. A.; Nemykin, V. N. Direct Synthesis of an Unprecedented Stable Radical of Nickel(II) 3,5-Bis (dimedonyl) azadiisindomethene with Strong and Narrow Near-Infrared Absorption at $\lambda \sim 1000$ nm. *Inorg. Chem.* **2017**, *56*, 6052–6055.
- (12) Feng, Y.; Burns, L. A.; Lee, L.-C.; Sherrill, C. D.; Jones, C. W.; Murdock, C. Co(III) Complexes of Tetradentate X3L Type Ligands: Synthesis, Electronic Structure, and Reactivity. *Inorg. Chim. Acta* **2015**, *430*, 30–35.
- (13) Sumiyoshi, A.; Chiba, Y.; Matsuoka, R.; Noda, T.; Nabeshima, T. Efficient Luminescent Properties and Cation Recognition Ability of Heavy Group-13 Element Complexes of N₂O₂- and N₂O₄-Type Dipyrins. *Dalton Trans.* **2019**, *48*, 13169–13175.
- (14) Sakakibara, K.; Takahashi, Y.; Nishiyabu, R.; Kubo, Y. A Zn²⁺-Coordinated Boronate Dipyrin as a Chemodosimeter toward Hydrogen Peroxide. *J. Mater. Chem. C* **2017**, *5*, 3684–3691.
- (15) Song, H.; Rajendiran, S.; Koo, E.; Min, B. K.; Jeong, S. K.; Thangadurai, T. D.; Yoon, S. Fluorescence Enhancement of N₂O₂-Type Dipyrin Ligand in Two Step Responding to Zinc(II) Ion. *J. Lumin.* **2012**, *132*, 3089–3092.
- (16) Zhou, X.; Yu, C.; Feng, Z.; Yu, Y.; Wang, J.; Hao, E.; Wei, Y.; Mu, X.; Jiao, L. Highly Regioselective α -Chlorination of the BODIPY Chromophore with Copper(II) Chloride. *Org. Lett.* **2015**, *17*, 4632–4635.
- (17) Kajiwar, Y.; Nagai, A.; Tanaka, K.; Chujo, Y. Efficient Simultaneous Emission from RGB-Emitting Organoboron Dyes Incorporated into Organic–Inorganic Hybrids and Preparation of White Light-Emitting Materials. *J. Mater. Chem. C* **2013**, *1*, 4437–4444.
- (18) Kubo, Y.; Minowa, Y.; Shoda, T.; Takeshita, K. Synthesis of a New Type of Dibenzopyrromethene–Boron Complex with Near-Infrared Absorption Property. *Tetrahedron Lett.* **2010**, *51*, 1600–1602.
- (19) Lakshmi, V.; Rao, M. R.; Ravikanth, M. Halogenated Boron-Dipyrromethenes: Synthesis, Properties and Applications. *Org. Biomol. Chem.* **2015**, *13*, 2501–2517.
- (20) Zhao, W.; Carreira, E. M. Conformationally Restricted Aza-Bodipy: A Highly Fluorescent, Stable, Near-Infrared-Absorbing Dye. *Angew. Chem.* **2005**, *117*, 1705–1707.
- (21) Zhao, W.; Carreira, E. M. Conformationally Restricted Aza-BODIPY: Highly Fluorescent, Stable Near-Infrared Absorbing Dyes. *Chem. - Eur. J.* **2006**, *12*, 7254–7263.
- (22) Luo, X.; Li, J.; Zhao, J.; Gu, L.; Qian, X.; Yang, Y. A general Approach to the Design of High-Performance Near-Infrared (NIR) D- π -A Type Fluorescent Dyes. *Chin. Chem. Lett.* **2019**, *30*, 839–846.
- (23) Zhu, X.; Lystrom, L.; Kilina, S.; Sun, W. Tuning the Photophysics and Reverse Saturable Absorption of Heteroleptic Cationic Iridium(III) Complexes via Substituents on the 6,6'-Bis(fluoren-2-yl)-2,2'-Biquinoline Ligand. *Inorg. Chem.* **2016**, *55*, 11908–11919.
- (24) Lu, T.; Wang, C.; Lystrom, L.; Pei, C.; Kilina, S.; Sun, W. Effects of Extending the π -Conjugation of the Acetylide Ligand on the Photophysics and Reverse Saturable Absorption of Pt(II) Bipyridine Bisacetylide Complexes. *Phys. Chem. Chem. Phys.* **2016**, *18*, 28674–28687.
- (25) Li, H.; Liu, S.; Lystrom, L.; Kilina, S.; Sun, W. Improving Triplet Excited-State Absorption and Lifetime of Cationic Iridium(III) Complexes by Extending π -Conjugation of the 2-(2-Quinoliny)-quinoxaline Ligand. *J. Photochem. Photobiol., A* **2020**, *400*, 112609–112623.
- (26) Monroe, S.; Scott, J.; Chouai, A.; Lincoln, R.; Zong, R.; Thummel, R. P.; McFarland, S. A. Photobiological Activity of Ru(II) Dyads Based on (Pyren-1-yl)ethynyl Derivatives of 1,10-Phenanthroline. *Inorg. Chem.* **2010**, *49*, 2889–2900.
- (27) Liu, B.; Monroe, S.; Li, Z.; Javed, M. A.; Ramirez, D.; Cameron, C. G.; Colón, K.; Roque, J., III; Kilina, S.; Tian, J. New Class of Homoleptic and Heteroleptic Bis(terpyridine) Iridium(III) Com-

plexes with Strong Photodynamic Therapy Effects. *ACS Appl. Bio Mater.* **2019**, *2*, 2964–2977.

(28) Liu, B.; Javed, M. A.; Guo, J.; Xu, W.; Brown, S. L.; Ugrinov, A.; Hobbie, E. K.; Kilina, S.; Qin, A.; Sun, W. Neutral Cyclometalated Iridium(III) Complexes Bearing Substituted N-Heterocyclic Carbene (NHC) Ligands for High-Performance Yellow OLED Application. *Inorg. Chem.* **2019**, *58*, 14377–14388.

(29) Wang, L.; Monro, S.; Cui, P.; Yin, H.; Liu, B.; Cameron, C. G.; Xu, W.; Hetu, M.; Fuller, A.; Kilina, S. Heteroleptic Ir(III)N₆ Complexes with Long-Lived Triplet Excited States and in vitro Photobiological Activities. *ACS Appl. Mater. Interfaces* **2019**, *11*, 3629–3644.

(30) Liu, B.; Monro, S.; Lystrom, L.; Cameron, C. G.; Colon, K.; Yin, H.; Kilina, S.; McFarland, S. A.; Sun, W. Photophysical and Photobiological Properties of Dinuclear Iridium(III) Bis-tridentate Complexes. *Inorg. Chem.* **2018**, *57*, 9859–9872.

(31) Zhu, X.; Cui, P.; Kilina, S.; Sun, W. Multifunctional Cationic Iridium(III) Complexes Bearing 2-Aryloxazolo [4,5-f][1,10] Phenanthroline (N⁺N) Ligand: Synthesis, Crystal Structure, Photophysics, Mechanochromic/Vapochromic Effects, and Reverse Saturable Absorption. *Inorg. Chem.* **2017**, *56*, 13715–13731.

(32) Copey, L.; Jean-Gérard, L.; Framery, E.; Pilet, G.; Andrioletti, B. Synthesis, Solid-State Analyses, and Anion-Binding Properties of meso-Aryldipyrrin-5,5-Diylbis(phenol) and -bis(aniline) Ligands. *Eur. J. Org. Chem.* **2014**, *2014*, 4759–4766.

(33) Nakano, K.; Kobayashi, K.; Nozaki, K. Tetravalent Metal Complexes as a New Family of Catalysts for Copolymerization of Epoxides with Carbon Dioxide. *J. Am. Chem. Soc.* **2011**, *133*, 10720–10723.

(34) Yamamura, M.; Takizawa, H.; Sakamoto, N.; Nabeshima, T. Monomeric and Dimeric Red/NIR-Fluorescent Dipyrrin–Germanium Complexes: Facile Monomer–Dimer Interconversion Driven by Acid/Base Additions. *Tetrahedron Lett.* **2013**, *54*, 7049–7052.

(35) Perdew, J. P.; Burke, K.; Ernzerhof, M. Generalized Gradient Approximation Made Simple. *Phys. Rev. Lett.* **1996**, *77*, 3865.

(36) Wadt, W. R.; Hay, P. J. Ab Initio Effective Core Potentials for Molecular Calculations. Potentials for Main Group Elements Na to Bi. *J. Chem. Phys.* **1985**, *82*, 284–298.

(37) Francel, M. M.; Pietro, W. J.; Hehre, W. J.; Binkley, J. S.; Gordon, M. S.; DeFrees, D. J.; Pople, J. A. Self-Consistent Molecular Orbital Methods. XXIII. A Polarization-Type Basis Set for Second-Row Elements. *J. Chem. Phys.* **1982**, *77*, 3654–3665.

(38) Krishnan, R.; Binkley, J. S.; Seeger, R.; Pople, J. A. Self-Consistent Molecular Orbital Methods. XX. A Basis Set for Correlated Wave Functions. *J. Chem. Phys.* **1980**, *72*, 650–654.

(39) Frisch, M. J.; Trucks, G. W.; Schlegel, H. B.; Scuseria, G. E.; Robb, M. A.; Cheeseman, J. R.; Scalmani, G.; Barone, V.; Petersson, G. A.; Nakatsuji, et al. *Gaussian 16 Rev. C.01*, Wallingford, CT, 2016.

(40) Barone, V.; Cossi, M.; Tomasi, J. Geometry Optimization of Molecular Structures in Solution by the Polarizable Continuum Model. *J. Comput. Chem.* **1998**, *19*, 404–417.

(41) Cossi, M.; Barone, V.; Cammi, R.; Tomasi, J. Ab Initio Study of Solvated Molecules: A New Implementation of the Polarizable Continuum Model. *Chem. Phys. Lett.* **1996**, *255*, 327–335.

(42) Liu, B.; Lystrom, L.; Brown, S. L.; Hobbie, E. K.; Kilina, S.; Sun, W. Impact of Benzannulation Site at the Diimine (N⁺N) Ligand on the Excited-State Properties and Reverse Saturable Absorption of Biscyclometalated Iridium(III) Complexes. *Inorg. Chem.* **2019**, *58*, 5483–5493.

(43) Liu, B.; Lystrom, L.; Kilina, S.; Sun, W. Effects of Varying the Benzannulation Site and π -Conjugation of the Cyclometalating Ligand on the Photophysics and Reverse Saturable Absorption of Monocationic Iridium(III) Complexes. *Inorg. Chem.* **2019**, *58*, 476–488.

(44) Liu, B.; Lystrom, L.; Kilina, S.; Sun, W. Tuning the Ground State and Excited State Properties of Monocationic Iridium(III) Complexes by Varying the Site of Benzannulation on Diimine Ligand. *Inorg. Chem.* **2017**, *56*, 5361–5370.

(45) Scalmani, G.; Frisch, M. J.; Mennucci, B.; Tomasi, J.; Cammi, R.; Barone, V. Geometries and Properties of Excited States in the Gas Phase and in Solution: Theory and Application of a Time-Dependent Density Functional Theory Polarizable Continuum Model. *J. Chem. Phys.* **2006**, *124*, 094107.

(46) Martin, R. L. Natural Transition Orbitals. *J. Chem. Phys.* **2003**, *118*, 4775–4777.

(47) Furche, F.; Ahlrichs, R. Adiabatic Time-Dependent Density Functional Methods for Excited State Properties. *J. Chem. Phys.* **2002**, *117*, 7433–7447.

(48) Van Caillie, C.; Amos, R. D. Geometric Derivatives of Density Functional Theory Excitation Energies Using Gradient-Corrected Functionals. *Chem. Phys. Lett.* **2000**, *317*, 159–164.

(49) Sifain, A. E.; Gifford, B. J.; Gao, D. W.; Lystrom, L.; Nelson, T. R.; Tretiak, S. NEXMD Modeling of Photoisomerization Dynamics of 4-Styrylquinoline. *J. Phys. Chem. A* **2018**, *122*, 9403–9411.

(50) Lystrom, L.; Zhang, Y.; Tretiak, S.; Nelson, T. Site-Specific Photodecomposition in Conjugated Energetic Materials. *J. Phys. Chem. A* **2018**, *122*, 6055–6061.

(51) Liu, B.; Javed, M. A.; Kilina, S.; Sun, W. Synthesis, Photophysics, and Reverse Saturable Absorption of trans-Bis-Cyclometalated Iridium(III) Complexes (C⁺N⁺C) Ir (R-tpy)⁺(tpy= 2, 2': 6', 2''-Terpyridine) with Broadband Excited-State Absorption. *Inorg. Chem.* **2020**, *59*, 8532–8542.

(52) Wang, L.; Yin, H.; Javed, M. A.; Hetu, M.; Wang, C.; Monro, S.; Zhu, X.; Kilina, S.; McFarland, S. A.; Sun, W. π -Expansive Heteroleptic Ruthenium(II) Complexes as Reverse Saturable Absorbers and Photosensitizers for Photodynamic Therapy. *Inorg. Chem.* **2017**, *56*, 3245–3259.

(53) Kasha, M. Characterization of Electronic Transitions in Complex Molecules. *Discuss. Faraday Soc.* **1950**, *9*, 14–19.

(54) Hilborn, R. C. Einstein Coefficients, Cross Sections, F Values, Dipole Moments, and All That. *Am. J. Phys.* **1982**, *50*, 982–986.